Large-Scale B3LYP Simulations of Ibuprofen Adsorbed in MCM-41 Mesoporous Silica as Drug Delivery System

Massimo Delle Piane, Marta Corno, Alfonso Pedone, Roberto Dovesi and Piero Ugliengo, Large-Scale B3LYP Simulations of Ibuprofen Adsorbed in MCM-41 Mesoporous Silica as Drug Delivery System, J. Phys. Chem. C, 2014, 118 (46), pp 26737–26749

Large-scale B3LYP simulations of ibuprofen adsorbed in MCM-41 mesoporous silica as drug delivery system

Massimo Delle Piane[1], Marta Corno[1], Alfonso Pedone[2], Roberto Dovesi[1], Piero Ugliengo[1*]

[1]*Department of Chemistry and NIS (Nanostructured Interfaces and Surfaces) Centre, University of Torino, via P. Giuria 7, 10125 Torino – Italy*

[2]*Department of Chemical and Geological Sciences, University of Modena and Reggio Emilia, via G. Campi 183, 41100 Modena – Italy*

[*]*Corresponding author: Phone: +39-011-6704596, Email: piero.ugliengo@unito.it*

Abstract

The atomistic details of the interaction between ibuprofen (one of the most common non-steroidal anti-inflammatory drug) and a realistic model of MCM-41 (one of the most studied mesoporous silica materials for drug delivery) have been elucidated by quantum mechanical modeling inclusive of London forces. Calculations are based on periodic Density Functional Theory (DFT) with the all-electron B3LYP hybrid functional. By docking the drug on different sites of the MCM-41 pore walls, we have sampled different local features of the potential energy surface of the drug-silica system, both for low and high loadings (1 and 7 drug molecules per unit cell, respectively). For all cases, ibuprofen adsorption in MCM-41 is exergonic (average ΔG = -33 kJ·mol^{-1}) and exothermic (average ΔH = -99 kJ·mol^{-1}), exclusively when London interactions are taken into account due to their dominant role in dictating all features of this system. The simulated IR and NMR spectra are in excellent agreement with the experiment and suggest an alternative interpretation to the current dynamic behavior of the adsorbed ibuprofen based on its static disorder due to surface sites heterogeneity. From these data, we also propose the existence of a synergic behavior in the H-bond donor/acceptor ability of the adsorbed drug. The present work shows that large-scale all-electron full quantum mechanical simulations employing accurate hybrid functionals can become soon competitive over modeling studies based on molecular mechanics methods, both in terms of superior accuracy and absence of the problematic parameterization due to organic/inorganic interface.

Keywords: Ibuprofen, mesoporous silica, B3LYP, B3LYP-D*, dispersion, adsorption, drug delivery, MCM-41, NMR.

1. Introduction

The interface between inorganic materials and fluids containing biologically relevant molecules like proteins is of extraordinary relevance[1-2] in medical devices, biotechnology and also in proteomics. Among the most important inorganic materials, silica-based ones play a key role, because they are chemically inert, structurally robust, easy to prepare and characterize. Considering silica-based materials, ordered mesoporous structures have attracted a great interest in the last decades since their discovery in the '90s.[3] They have found many applications in separation, catalysis, sensors and devices.[4] Generally, they show a regular (ordered) arrangement of either cylindrical pores or cages of mesoporous size (2-10 nm) with high surface area. The structure of the pore wall consists of a disordered network of siloxane bridges and silanol groups (SiOH) at the surface.[5] As drug delivery systems they are compatible with the fundamental requirements of biodegradability and biocompatibility. Since the first report by Vallet-Regi *et al.* in 2001[6] using MCM-41 as a new drug delivery system, a large number of investigations have been conducted in this area.[7-8] Detailed lists of drug/mesoporous-solid systems are reported in Ref.[7-9] Among drugs, the most studied one is ibuprofen, a common non-steroidal anti-inflammatory drug.[10] Obviously, the adsorption of drugs into the pores is a surface phenomenon governed mainly by interactions between silanol groups and the functional groups of the guest molecules, but also London type (or dispersion) interactions can play an important role considering the hydrophobic nature of ibuprofen. An interesting point of debate in the study of ibuprofen confinement in mesoporous silica concerns the physical state of this molecule in the system. In particular, it is still not clear if the majority of the drug population is in interaction with pore walls or in a free state and, in this case, if as a free molecule or in a dimeric form. Initial NMR results suggested that ibuprofen exists in a high mobility

state when confined in mesoporous silica[11-13]. It was even claimed that it has a liquid-like behavior, similar to a super-cooled liquid. Very recently, the same research group confirmed their results through MAS-PFG NMR and hyperpolarised-^{129}Xe NMR spectroscopy, even estimating the diffusion coefficient of the drug when inside MCM-41 pores.[14] From these results, some researchers have inferred that ibuprofen is mainly in a non-interacting state. One possible explanation to this is that ibuprofen is in its dimeric form as shown by the absence of the OH bands due to the strong H-bond. Indeed, molecular dynamics simulations have demonstrated that dimers are the main sub-population when this molecule is in a super-cooled liquid state.[15] More recently, relaxation dielectric spectroscopy studies[13,16] have revealed a more complex scenario with two main families with different mobility: one group corresponds to molecules free to move in the center of the pore (existing mainly as dimers and with a mobility higher than bulk ibuprofen), while the other is composed of molecules in interaction with pore walls, whose mobility is therefore constrained. Ref.[14] also suggests this, by obtaining two distinct diffusion coefficients for ibuprofen in MCM-41. From this experimental evidence it can be suggested that pore diameter and, most importantly, surface features may influence the distribution of drug molecules between the two families.

From the above illustrated points, it is clear that a detailed and accurate model of MCM-41 is needed with the purpose to simulate quantum mechanically the processes of interest at the atomic level. Recently, some of us have proposed a realistic model for MCM-41 bulk material[17]. This structure presents holes of diameter of about 30 Å and walls about 10 Å thick, with the OH density around 7 OH/nm^2. This model has recently been checked against a variety of physical observable, *i.e*. simulated x-ray diffraction, small angle neutron scattering and electronic microscopy, showing good agreement

with experimental data.[18] This ensures that the MCM-41 model can be adopted to study more challenging problems such as the adsorption of optically active molecules[19] and/or drugs. As for drug interactions, some of us have very recently successfully modeled[20] aspirin and ibuprofen adsorbed on extended amorphous silica surfaces (1.5 and 4.5 OH/nm^2) models, also defined in Ref.[17]. It was shown that the obtained interaction energies were a delicate balance between H-bonds and London forces.

In the present paper we extend the drug/excipient study by focusing exclusively on the interaction of ibuprofen with the internal walls of MCM-41. In particular, our objectives were: i) to quantify how different the energy of interaction is as a function of the ibuprofen adsorption in different MCM-41 internal surface sites; ii) to study the thermodynamics of the drug-mesoporous silica system and iii) to simulate IR and NMR spectra to interpret experimental measurements on the atomistic base. The latter is a key point in order to validate our results by comparison with experimental data. The adopted approach is based on well know quantum mechanical methods based on DFT with an *a posteriori* dispersion correction (B3LYP-D*)[21] to check the role of London forces in such systems.

2. Computational Details

The development version of the CRYSTAL14 code has been adopted for all the ab-initio calculations[22] in its massively parallel implementation.[23-24]

2.1 Hamiltonian

All the calculations have been performed within the Density Functional Theory (DFT) adopting the Becke, 3 parameters, Lee-Yang-Parr (B3LYP) hybrid functional.[25-26] B3LYP is still recognized as one of the most widely used and well balanced functional as for its accuracy due to the enormous database of results accumulated over the years.

The present implementation in CRYSTAL is very efficient compared to other codes based on plane waves, being only about three times slower than pure GGAs. The electron density and its gradient were integrated over a pruned grid consisting of 974 angular and 75 radial points generated through the Gauss–Legendre quadrature and Lebedev schemes.[27] Values of the tolerances that control the Coulomb and exchange series in periodical systems[28] were set to 10^{-6} and 10^{-16} Ha. For all calculations, the Hamiltonian matrix was diagonalized using 8*k* points (shrinking factor = 2).[29] The eigenvalue level-shifting technique was used to lock the system in a non-conducting state,[28] with level shifter set to 0.6 Ha. To help convergence of the SCF, the Fock/KS matrix at a cycle was mixed with 30% of the one of the previous cycle.[28]

2.2 Basis set

The same split valence double- and triple-ζ basis set *plus* polarization functions employed in Ref.[20] has been applied here to describe the majority of the elements. The original choice was aimed at reducing the BSSE error and the same demand still applies here. Different basis sets were employed to describe the atoms of the silica framework and those of ibuprofen, balancing precision and computational cost of the calculations. Considering MCM-41, Si atoms were represented by a 88-31G* basis set and O atoms were described by a 8-411G* basis set, both by Nada,[30] while for H atoms we employed a 3-11G* VTZd set by Ahlrichs.[31] Ibuprofen atoms were all described by the VTZd basis set by Ahlrichs:[31] a 511111-411G* basis set for C and O and the same 3-11G* set for H used for the silica surface.

2.3 Geometry optimization

Internal coordinates have been optimized using the analytical gradient method. The Hessian is upgraded with the Broyden-Fletcher-Goldfarb-Shanno (BFGS) algorithm.[32-34] Tolerances for the maximum allowed gradient and the maximum atomic

displacement for convergence have been kept at the default values (0.00045 Ha·bohr^{-1} and 0.00030 bohr, respectively). To compensate the reduced thickness of the pore walls, in the docking models only the drugs and the surface OH groups have been moved, while keeping the rest of the silica framework and the cell parameters fixed at its optimized geometry (free from ibuprofen adsorption). The largest considered system (MCM-41 in interaction with 7 ibuprofen molecules) includes 810 atoms in the unit cell (for a total of 12054 atomic orbitals).

2.4 Vibrational frequencies

Harmonic frequencies were calculated with CRYSTAL in Γ point and the infrared intensity for each normal mode was obtained by computing the dipole moment variation along the normal mode, adopting the Berry phase method.[35] The default value of 0.003 Å has been chosen as the displacement of each atomic coordinate and the tolerance for the SCF cycle convergence has been tightened from 10^{-6} (default value) to 10^{-11} Ha. For the simulation of the IR spectrum of the MCM-41 material, only a fragment consisting of the surface OH groups has been considered for constructing the Hessian matrix. In both the cases with crystalline ibuprofen and with the molecule adsorbed inside the pores, the vibrational analysis has been limited to the COOH group of the drug, since experimental results only focused on the C=O stretching frequency. In this last case, the IR intensities were not computed. To compute thermodynamic data, a vibrational analysis of a fragment including all 33 atoms of the molecule has been performed both for molecular ibuprofen and for one adsorption case (S1, *vide infra*).

2.5 NMR chemical shifts

The ^{1}H and ^{13}C shielding tensors were computed by means of the Gauge Including Projection Augmented Wave (GIPAW) approach[36-37] encoded in the Quantum Espresso package[38] which uses Plane Waves as basis-set and the pseudo-potential approach to

describe the core-valence interactions. As the hybrid functionals are not efficiently implemented in plane waves based codes, particularly for systems of the present case, the PBE exchange-correlation functional[39] has been used in all the calculations without including dispersion-correction terms and run on the B3LYP-D* optimized structures. The latter are *a posteriori* empirical corrections to the DFT energy and forces and thus they do not directly affect the computation of the NMR parameters. Vanderbilt UltraSoft PseudoPotentials[40] included in the QE library were used for Si and O nuclei whereas the Rappe Rabe Kaxiras Joannopoulos US PP[41] properly generated for GIPAW calculations were used for C and H atoms. The Plane Wave basis-set was cut at 1090 eV.

The ^{13}C and ^{1}H isotropic chemical shift (δ_{iso}) were derived from the isotropic shielding through the following relations:

$$\delta_{iso}(^{13}C) = -0.9334\sigma_{iso} + 163.4 \quad (1)$$

$$\delta_{iso}(^{1}H) = -0.9494\sigma + 28.804 \quad (2)$$

which were fitted on the measured isotropic chemical shift of the 1α crystal phase of the half sandwich Ru(II)-complex [(p-cymene)Ru(kN-INA)Cl_2] (INA = isonicotinic acid) molecule, that was investigated in a previous paper and taken as reference.[42] The linear regression shown in Figure S1 of Supporting Information yielded R^2 of 0.9954 and 0.9697 for ^{13}C and ^{1}H, respectively.

The computed ^{13}C isotropic chemical shifts were then used to simulate the corresponding MAS NMR spectra of all the structures, by means of a home-made code based on the resolution of spin effective Hamiltonians similar to the fpNMR code previously described.[43]

The ^{1}H MAS NMR spectra were not simulated because the broadening effects due to the homonuclear dipole-dipole interactions, which are not averaged out in the

experimental spectra reported in literature,[11] are not included in the present version of our code.

2.6 Calculation of interaction energies

The energetics of the drug-silica system has been studied using the same expressions of Ref.[20], adapted to work for a 3D mesoporous silica framework. A detailed description of the formulas used in these calculations is reported in Supporting Information.

Enthalpy (ΔH), entropy (ΔS) and free energy (ΔG) of adsorption at standard temperature (298 K) were obtained from the vibrational partition function of the ibuprofen molecule only, *i.e.* assuming zero contribution from the vibrational internal modes of the silica framework. Notwithstanding this simplification, a full vibrational analysis of the molecule, both free and when adsorbed, is still required to compute the partition function for all considered cases. To save computer time, the procedure has been limited to the S1 adsorption geometry and the obtained Zero Point Energy (ΔZPE) and thermal (ΔE_T) corrections to the BSSE corrected electronic adsorption energy (ΔE^C) were applied to all other cases, as:

$$\Delta H = \Delta E^C + \Delta ZPE + \Delta E_T \qquad \Delta G = \Delta H - T\Delta S \tag{3}$$

2.7 Dispersion correction

A general drawback of most common DFT functionals, including hybrids, is that they cannot describe long-range electron correlations that are responsible for van der Waals (dispersive) forces. Since dispersion plays a key role in many chemical systems, particularly in determining the orientation of molecules on surfaces, it was necessary to correct the energy obtained with the standard density functional methods. When dispersion is included in the system, the total computed energy is given by:

$$E_{DFT\text{-}D} = E_{DFT} + E_{disp} \tag{4}$$

where E_{disp} is the empirical dispersion correction originally proposed by Grimme[21] and known as D2 correction with the modification proposed by Civalleri *et al.* to the standard set of parameters for calculations using the B3LYP hybrid functional.[44] This correction will be referred in the following with the D* labeling. When activated during a geometry optimization, it was added to the energy and its gradient to determine the final geometry. All the terms in the equations to compute the interaction energies can be written including the dispersion contribution (in the following, it is expressed by the D superscript). However, since this correction does not depend on the basis set, the dispersion contribution is not affected by the BSSE and the counterpoise method has been applied only on the purely DFT part of the energy. Dispersion interactions do indeed affect the BSSE in an indirect way, as the final geometries are affected by the dispersion interactions.

3. Results and discussion

3.1 The MCM-41 model

A model for the mesoporous silica material MCM-41 has already been proposed and described by some of us.[17] Briefly, it was obtained by amorphizing a hexagonal supercell of α-quartz through classical molecular dynamics at high temperature, then manually excavating the pore, saturating all the dangling bonds with H atoms and finally optimizing the obtained structure with DFT. For the purpose of the present paper, this MCM-41 model has been re-optimized at both B3LYP/TVZ and B3LYP-D*/TVZ levels of theory. Figure 1 (Left) shows the unit cell of the B3LYP-D* optimized model, with resulting cell size $a = b = 40.6$ Å and $c = 12.2$ Å (indeed, Kresge *et al.*, in their first paper reporting the synthesis of the MCM-41 material,[3] describe an hexagonal unit cell with $a \approx 40$ Å) and containing 579 atoms ($Si_{142}O_{335}H_{102}$). In Figure

1 (Right) the crystalline packing is reported so to highlight the hexagonal arrangement of the pores of this class of materials. For this model, the pores have a diameter of *circa* 30 Å, in agreement with experimental samples,[3,11,18] and their walls thickness is 8-9 Å, close to the usual experimental values reported in the literature.[18] The surface density of silanol groups is 7.2 OH·nm^{-2}. This value is typical for silica surfaces cut from a bulk and saturated with H atoms, but larger than the typical silanol density for silica samples outgassed at ~200 K, that is 4.9 OH·nm^{-2}.[45]

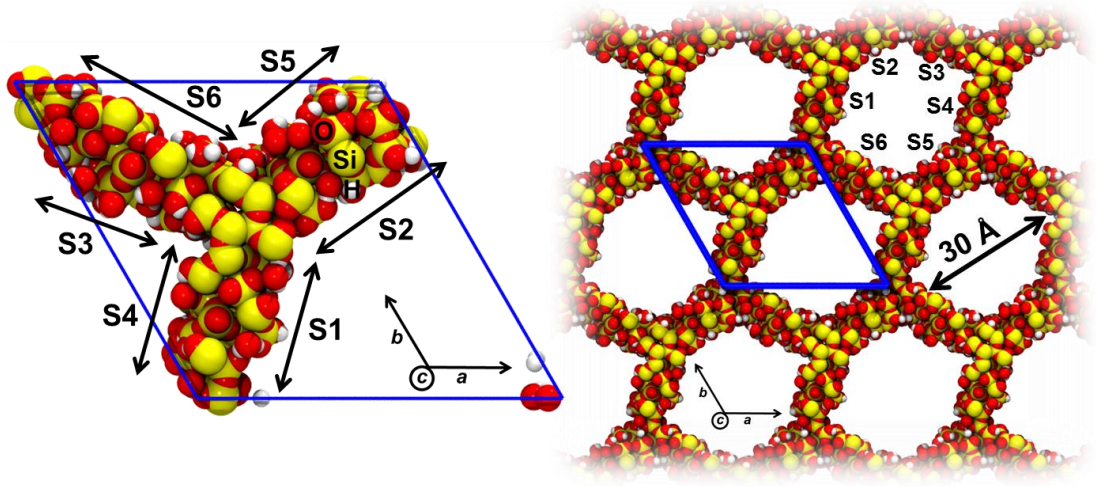

Figure 1. The MCM-41 model (B3LYP-D*). Left: unit cell ($Si_{142}O_{335}H_{102}$, $a = b = 40.6$ Å, $c = 12.2$ Å). Right: crystal packing. Both views along the *c* axis. Cell borders in blue. The six internal wall faces are identified as S1-6.

This MCM-41 model has been already successfully validated against many experimental observables in Ref.[18]: X-ray diffraction, small angle neutron scattering and transmission electron microscopy have been simulated; chord length distributions, surface smoothness/roughness, porous volume and geometrical surface have been determined and Grand Canonical Monte Carlo has been employed to study the adsorption of N_2, CO_2, and H_2O.

In the present paper, we further extend this analysis by reporting the B3LYP-D* simulated infrared IR vibrational spectrum of the material (Figure 2). We focused

on the stretching modes of the surface OH groups that constitute the main features of a silica surface which allows to monitor the perturbations induced by the adsorbed molecules. It is well known that hydrogen bonding has a strong effect on infrared spectra, not only by causing a bathochromic shift of the stretching frequencies for the involved groups, but also by broadening the corresponding spectral bands. This latter effect is not encoded in standard *ab initio* programs. To compare our simulated data with experimental ones, however, an empirical correction[46] has been adopted to correlate the calculated IR bathochromic shift of the surface OH groups with the band width. This approach has already been successfully employed in the past by some of us to reproduce the vibrational spectrum of hydroxylated crystalline edingtonite silica faces.[47] Figure 2 reports the comparison between our simulated spectrum (blue) and an experimental one[48] for a micelle-templated silica sample (blue). To account for the deviation of the OH stretching mode from being a harmonic oscillator, the single scaling factor 0.960 was applied to all derived B3LYP-D* ν(OH) values. The agreement is remarkable. The clear band at ~3740 cm^{-1} is due to non-interacting isolated silanols while the very large band at lower wavenumbers is the result of all the silanols that take part into H-bond interactions. The good agreement between experimental data and this spectrum, together with previously reported results[18], demonstrates that our MCM-41 model is indeed a good representation of the "real" material and is a trustworthy starting point to follow the adsorption of drugs on its pore walls.

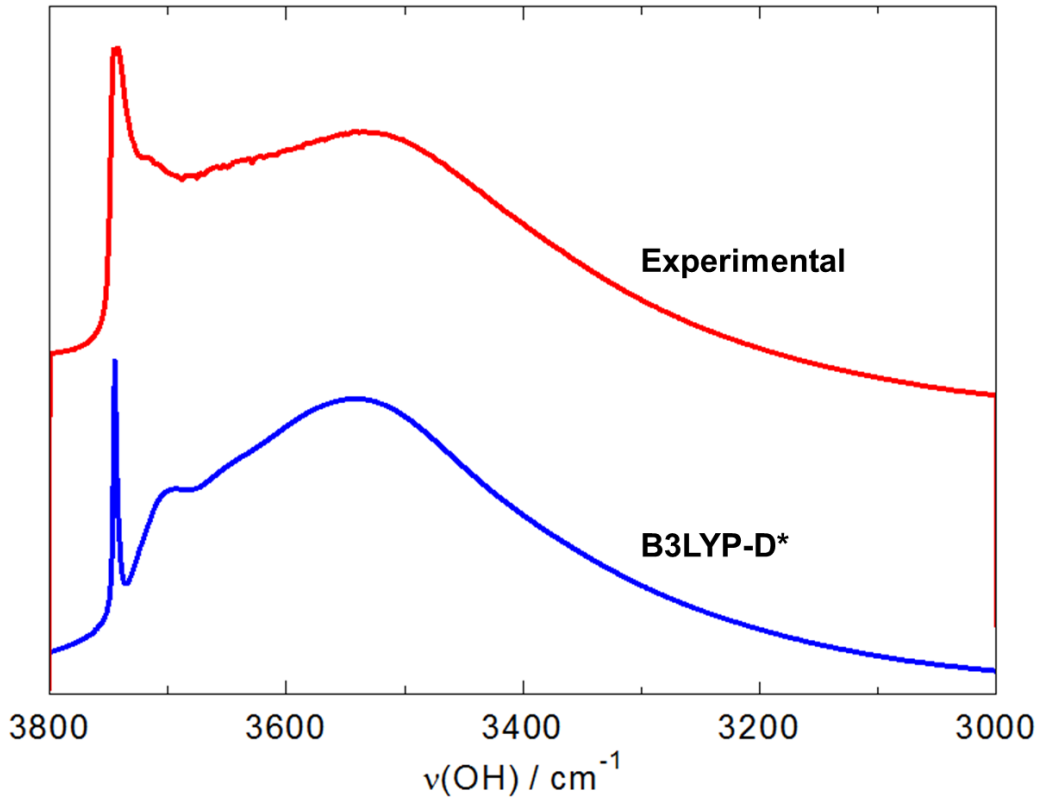

Figure 2. Experimental[48] (top, red) and simulated B3LYP-D* (bottom, blue) infrared spectra of MCM-41in the OH stretching frequency region.

In the past, we have already studied the adsorption of drugs on models of silica surfaces.[20] The MCM-41 case, however, adds complexity to the study because it consists of a 3D silica framework with an intricate pore wall morphology. To simplify the sampling of the potential energy surface of ibuprofen adsorption in such a complex material, a "divide & conquer" strategy has been followed, by subdividing the pore wall into six "faces" and treating them as six separate adsorption zones. This approach allows to treat drug adsorption in MCM-41 in the same way as for silica surfaces.[20] These six inner surfaces, hereafter named S1-6, are defined in Figure 1 and they are viewed in more detail in Figure 3. As expected, in all cases the most prominent surface feature is represented by SiOH functionalities (silanols). The high hydroxylation level of the pore walls, as stated above, results in a large network of H-bond interactions

between these groups. Indeed, in our model, only 33 of the total 102 SiOHs are not involved in H-bonds. Furthermore, the way this model has been generated results in a large number of geminal silanols, *i.e.* silicon atoms connected to two OH groups. Long chains of H-bonds are known to be particularly stable surface features[5] and the high silanol density of this model produces long chains, that are particularly evident on S1 and S3. Despite the abundance of silanols, some of them are clearly not available for interaction with an approaching molecule, being not exposed to the surface and/or involved in interactions with siloxane bridges (-Si-O-Si-) of the underlying silica framework.

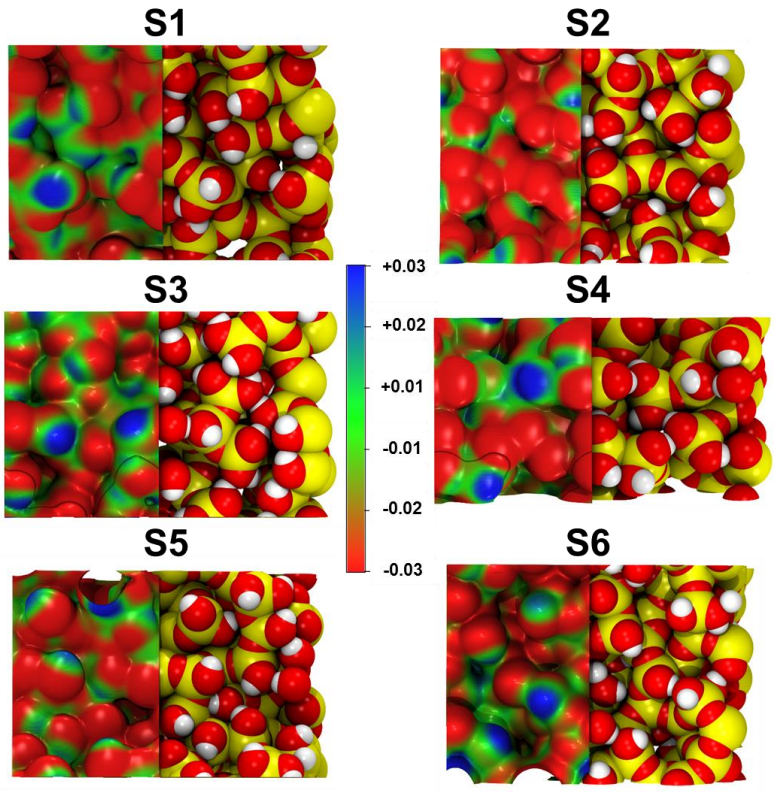

Figure 3. The six S1-6 inner faces of the MCM-41 pore walls. The right strip shows the space filled structure on top of which (left strip) the electrostatic potential is mapped on the electron density isosurface (isovalue: 0.0004 *e*). Color scale shown in the picture.

One way to foresee the most favorable adsorption spots is to seek complementarity between the electrostatic potential of the surface and that of the

incoming molecule. Figure 3 reports the electrostatic potential mapped on the electron density of the six S1-6 faces. In the figure, blue represents a positive value of the potential, red a negative one and green neutrality. A general negative character due to silanol oxygens is clear, particularly for S2. Terminal silanol hydrogens are associated to positive values of the potential, with increasing positivity as a function of the H-bond chain length. This increases the Brønsted acidity of silanol groups which are terminal of an H-bonded chain. This is especially evident on the S1 surface. Neutral basins are rare and are due to parts of the silica framework more exposed at the surface. These maps indicate that the whole inner surface of the pore is apt to adsorb molecules that expose polar functionalities, like the COOH group of ibuprofen, acting both as a strong donor and acceptor of H-bonds and being adsorbed through electrostatic complementarity.

3.2 Ibuprofen adsorption: Single Loading

Initially, the interaction between ibuprofen (2-(4-isobutylphenyl)-propionic acid ($H_{18}C_{13}O_2$)) and MCM-41 was probed by adsorbing one drug molecule on each one of the six faces identified on the pore walls. Starting geometries were mainly determined by electrostatic complementarity.

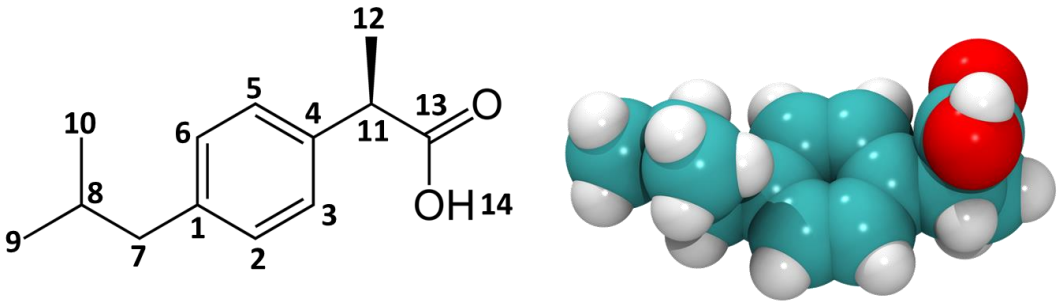

Figure 4. Structure of the 2-(4-isobutylphenyl)-propionic acid ($H_{18}C_{13}O_2$), ibuprofen drug molecule. Left: 2D chemical structure with atom numbering. Right: 3D space filling model of the B3LYP-D* optimized most stable conformer.

Ibuprofen (Figure 4) is largely an apolar molecule[49] (logP=3.8), due to its methylpropylphenyl part, except for the propanoic acidic functionality[50] (pKa = 4.3) that exhibits both negative (on oxygens) and positive (on carboxylic hydrogen) electrostatic potential values. It is therefore expected (and confirmed by both theoretical[20] and experimental[11,51] results) that adsorption of ibuprofen on silica-based materials will be driven by its polar head, with the rest of the molecule involved in non-specific dispersion driven interactions. Accordingly, in the present work, ibuprofen has been docked trying to form stable H-bond interactions between its COOH group and available surface silanols (favoring those particularly acidic or basic as being part of long H-bond networks on the surface) and by maximizing the contact between the rest of the molecule and the material. All structures were optimized both with (B3LYP-D*) and without (B3LYP) dispersion contribution to the energy (see Computational Details) to highlight its role in these adsorption events. Note that in the optimization process, only the surface OHs have been allowed to move, while keeping the coordinates of the rest of the silica framework and the cell size fixed. This was done: i) to greatly reduce the degrees of freedom of the system, allowing for a faster convergence in the optimization; ii) to compensate for the reduced thickness of the pore walls in cases of adsorption at higher ibuprofen loading in which the perturbation on the wall can be exceedingly large.

The six resulting B3LYP-D* models, at a loading of 1 molecule/pore, are reported in Figure 5, as space-filled structures and, in Figure 6, focusing on the details of the H-bond interactions.

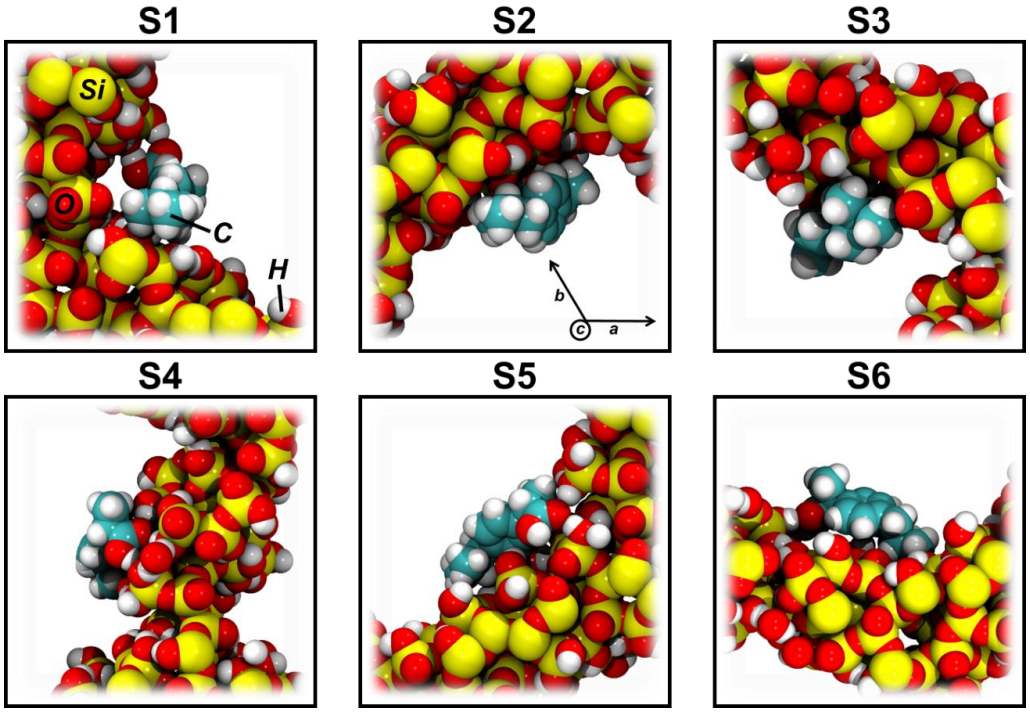

Figure 5. Space filled views along the *c* axis of the six S1-6 B3LYP-D* models of one ibuprofen molecule adsorbed on the MCM-41 pore walls. Only the area of interest is shown in each case.

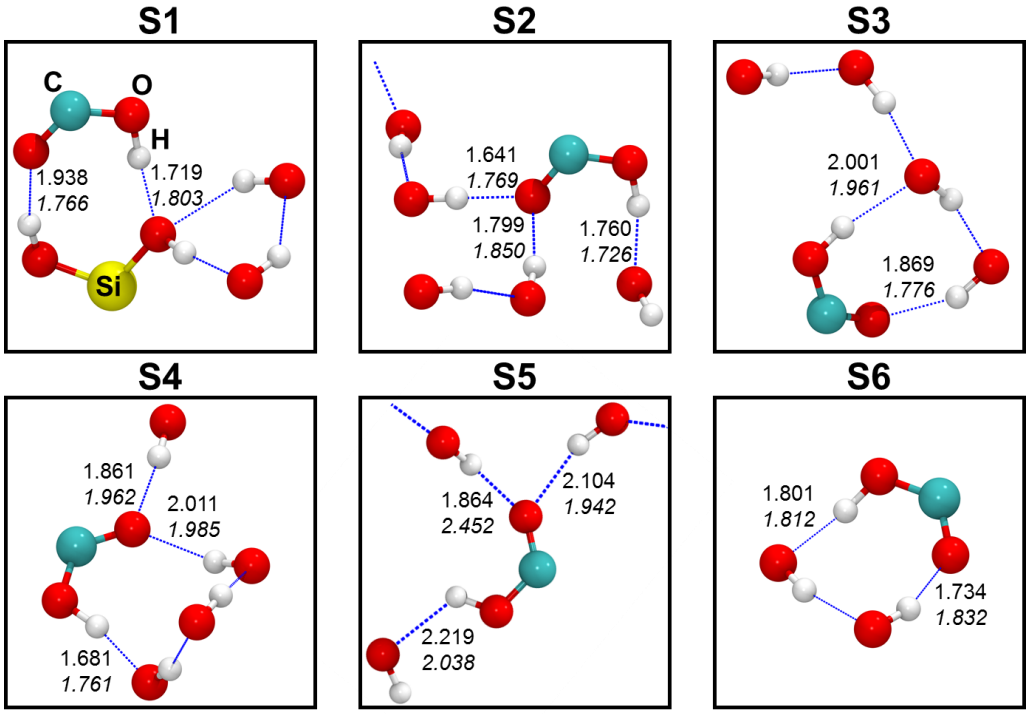

Figure 6. Details of the interaction between ibuprofen and MCM-41 pore walls for the six S1-6 B3LYP-D* models of Figure 5. Only the drug COOH group and the OH groups of the involved silanols are shown for better clarity. H-bonds are dashed blue lines and

their lengths for selected interactions are reported in Å: upright values are for B3LYP-D* optimized structures, while values in italics are for B3LYP optimized structures (without dispersion).

We will not describe here in details each adsorption structure, because it would be uninformative. Since the real mesoporous silica material is amorphous, none of these geometries is expected to be actually present in a real sample exactly in this form. Indeed, the purpose of the present work is to shed light on the general mechanism of interaction between drugs and mesoporous silicas, identifying the driving forces behind the process.

On average, ibuprofen forms 2.3 H-bonds between COOH group and the surface (Figure 6). In all cases the hydrogen and the carbonyl oxygen are involved in the interaction (average H-bond length is 1.864 Å and 1.840 Å, respectively). The latter may accept one or two bonds, depending on the structure, through its lone pairs. The oxygen of the OH group is never detected in specific interactions during the adsorption process. In most cases, silanols under the molecule are seen forming weak interactions with its phenyl ring. This is particularly evident for adsorption on the S5 face (Figure 5). Although these interactions surely contribute to the stability of the adsorption, we do not consider them driving forces of the process, since they appear mostly as an "after-effect" of a structure already formed and stabilized by other dominating interactions.

In S3, S4 and S6 the interaction involves the formation of H-bond rings of general structure: OH_{ibu}---OH_{Si}---(OH_{Si})---OH_{Si}---OC_{ibu}. These motives were already observed for ibuprofen interacting with an hydroxylated amorphous silica surface[20] and may be particularly stabilizing since a proton relay mechanism may occur resulting in

different final proton sequence. However, this process cannot be seen in our static simulations and will be subject to further study.

Adsorption on the S2 structure is of particular interest, because the ibuprofen carbonyl oxygen is acceptor of an H-bond from a silanol that is terminal of a very long chain (only its terminal moiety is shown in Figure 6). This results in the shortest (therefore, strongest) H-bond of all considered models, with a B3LYP-D* length of 1.641 Å. Furthermore, Figure 3 shows that such a long chain of interacting silanols was not originally present on S2: this indicates that the surface has undergone a profound rearrangement in response to ibuprofen adsorption. This phenomenon is confirmed by calculating the deformation cost of the MCM-41 material (δE_M). As reported in Table S1, this contribution is repulsive and amounts to 33.5 kJ·mol^{-1} (B3LYP-D*) close to the one calculated for the S4 case (34.3 kJ·mol^{-1}) where a similar deep rearrangement of the surface silanols is observed to maximize the interactions with the ibuprofen molecule. Apart from these specific situations, silica deformation costs are large in all cases, averaging 22 kJ·mol^{-1}, reflecting a known high O-Si-O-H torsional mobility of surface silanols[5] that lets the surface to adapt to the incoming molecules.

In the same way silica responds to the incoming molecule, also the latter adapts to stabilize the interaction. Structures of Figure 5 correspond to the B3LYP-D* optimized models: in all cases it is evident that ibuprofen maximizes its contact with the wall, particularly by rotation of the dihedrals corresponding to the two methylpropylphenyl and propanoic substituents. Rotations up to 31° and 37°, respectively, are observed with respect to optimized ibuprofen in gas phase. This corresponds to an average B3LYP-D* deformation cost for the molecule of 12.6 kJ·mol^{-1} (ΔE_I in Table S1).

3.3 Ibuprofen adsorption: High Loading

The models with one adsorbed ibuprofen molecule per pore described up to now are certainly informative in understanding the atomistic principles of drug adsorption in mesoporous silica. However, the molecular picture they represent is quite far from the real incorporation of the drug in MCM-41.

To move towards a realistic description of what happens in such formulations, we have increased the ibuprofen loading up to seven molecules/pore. The B3LYP-D* structure is reported in Figure 7, both viewed along the *c* axis and cut to see the pore walls. To generate this model, we have merged the six structures of Figure 5 (here named HL-1 to 6). Furthermore, to compensate for a still large unoccupied surface area on the walls, a seventh molecule (HL-7) has been adsorbed on the S1 face. The final structure exhibits an almost uniform coverage of the pore surface (Figure 7, left).

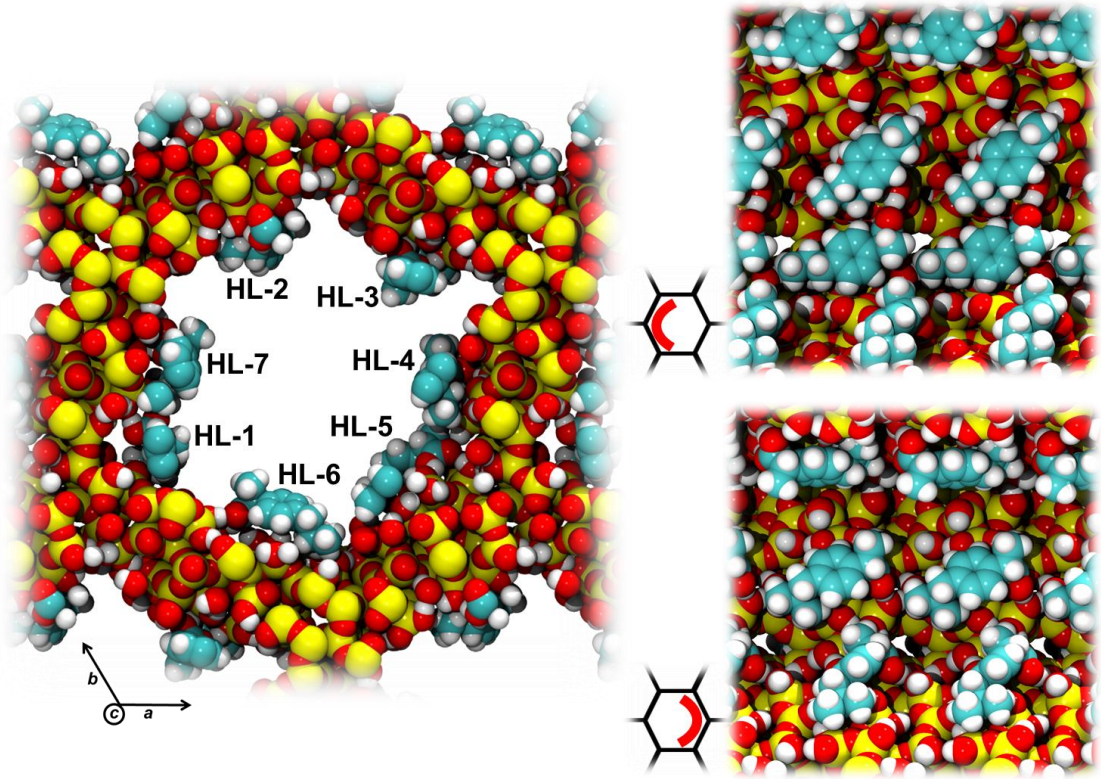

Figure 7. B3LYP-D* structure of the High Loading model, *i.e.* MCM-41 with seven ibuprofen molecules adsorbed in its pore. Left: view along *c* axis; right: lateral view cut to show the two halves of the pore.

The High Loading model corresponds to an ibuprofen incorporation of about 152 $mg \cdot g^{-1}$ (ibuprofen/silica). This value is still far to that reported experimentally after a full incorporation procedure. Babonneau and coworkers[11] mention an incorporation of 670 $mg \cdot g^{-1}$ for a sample of MCM-41 with a pore diameter of 35 Å (thus very close to the pore diameter for the MCM-41 model). However, they also suggest a complete pore occlusion, corresponding, for our model, to about 30 molecules per pore (of which 15 required to the formation of a monolayer). The resulting system size (*circa* 1600 atoms) would be about two times larger than our High Loading model (810 atoms) and, despite being doable, is beyond the scope of the present work.

Nevertheless, the model of Figure 7 is still instructional about the phenomena occurring in such systems. A comparison between this structure and the Single Loading cases of Figure 5 reveals that little movements occur when the different arrangements are put together. This suggests that at the present loading the adsorption sites are still almost independent from each other, with limited lateral interactions between ibuprofen molecules. However, an impending clustering of the molecules is seen on faces S1-S6 (Figure 7, top right): three ibuprofens reorient their apolar portions, in order to maximize the intermolecular vdW attraction. As in the Single Loading cases, B3LYP-D* brings all molecules significantly closer to the silica wall than with pure B3LYP (not shown here).

3.4 Energetics of the interaction and role of dispersion

In considering the adsorption energies for the modeled adsorption geometries, it is important to stress the significance of energies computed by including/excluding the dispersive interactions. In the case of B3LYP calculations, the only driving force for the drug-silica interaction is the formation of hydrogen bonds between silanols and the

carboxylic group of the molecule (and, partly, the phenyl ring). The rest of the ibuprofen molecule is subject to steric repulsion with respect to the underlying silica surface. Therefore, the final B3LYP optimized structures and the computed interaction energies result from a balance of these two effects. On the other hand, inclusion of dispersion interactions, via the Grimme's empirical correction, dramatically changes the above scenario by contrasting the pure electronic repulsion and becoming a significant fraction to the adsorption energy.

Table 1. Energetics of the ibuprofen/MCM-41 interaction. S1-6 refer to the six Single Loading structures, while High Loading refers to the model with seven drug molecules adsorbed into the pore. ΔE^{C} is the electronic interaction energy, without accounting for dispersion, corrected for BSSE (see Supporting Information). ΔE^{CD} is the electronic interaction energy, accounting for dispersion. DISP is the dispersion contribution, evaluated as ΔE^{CD}- ΔE^{C}. ΔH^{D} and ΔG^{D} are the enthalpy and free energy of adsorption (dispersion included), respectively (T=298 K). The description of how the latter thermodynamic quantities have been computed can be found in Computional Details. All energy values are in $kJ \cdot mol^{-1}$.

SYSTEM	**ΔE^{C}**	**ΔE^{CD}**	**DISP**	**ΔH^{D}**	**ΔG^{D}**
S1	-49.1	-107.8	54%	-99.2	-33.5
S2	-46.8	-121.7	62%	-113.1	-47.4
S3	-40.4	-90.8	56%	-82.3	-16.6
S4	-38.1	-99.5	62%	-90.9	-25.2
S5	-36.3	-122.4	70%	-113.8	-48.2
S6	-40.0	-100.0	60%	-91.5	-25.8
Average	*-41.8*	*-107.0*	*61%*		
St. Deviation σ	*5*	*13*	*6%*		
High Loading	-39.9	-105.6	62%	-97.0	-31.3

Table 1 reports the adsorption energies of ibuprofen inside the MCM-41 pore (Single and High Loadings), both B3LYP (ΔE^{C}) and B3LYP-D* (ΔE^{CD}), together with related thermodynamic quantities (ΔH^{D}, ΔG^{D}). Furthermore, Tables S1 and S2 (Supporting Information) report, for all structures, the various contributions to the interaction energy, both with and without dispersion. All values in Table 1 are BSSE corrected, for energies before correction refer to Supporting Information.

3.4.1 Single Loading

Considering Single Loading, all values are negative, suggesting that all bound structures are favored over the unbound molecule and silica, regardless of the adsorption site. A first, remarkable, consequence of the inclusion of Grimme's correction is the difference, for all models, between the B3LYP and B3LYP-D* computed values. The average B3LYP adsorption energy is -41.8 kJ·mol^{-1} while by including dispersion increases to -107.0 kJ·mol^{-1}, a dramatic +156% gain. From these numbers we deduced that: i) dispersive forces contribute, on average, for about 61% of the total interaction energy (thus constituting the main driving force of ibuprofen adsorption); ii) modeling such systems by means of standard DFT functionals lacking the inclusion of these forces results in a rough description of their energetics.

B3LYP interaction energies are consistent with the energies of 2-3 H-bonds.[52] Despite a significant variability between the interaction patterns, as shown in Figure 6, the corresponding adsorption energies are very close to each other (standard deviation, $\sigma \pm 5$ kJ·mol^{-1}). This suggests a certain equivalency between adsorption sites on MCM-41 walls, at least as regards the H-bond formation. The larger interaction energies correspond to models S1 and S2 (-49.1 and -46.8 kJ·mol^{-1}, respectively). For the former, Figure 6 points to a possible stabilizing role of the ring pattern that includes one silanol interacting with ibuprofen. S2, on the other hand, is stabilized by the above mentioned

formation of a long network of interacting silanols. Conversely, S5 is the least stable structure (-36.3 kJ·mol^{-1}) and indeed Figure 6 reports the longest H-bond distances (B3LYP values in italics) among the models.

B3LYP-D* interaction energies are not only much larger than those without dispersion, as pointed out above, but are also significantly more disperse ($\sigma \pm 13$ kJ·mol^{-1}). Introduction of vdW interactions changes the Potential Energy Surface (PES) of the drug-silica system and makes it "rougher", increasing the differences between the various adsorption sites. Interestingly, when considering dispersion, the most stable structure becomes S5 (-122.4 kJ·mol^{-1}), that was the least favorable according to pure B3LYP. Figure 5 shows that ibuprofen on S5 is adsorbed sideways, extending the contact between the alkyl substituent and the surface. This structure displays the highest dispersion contribution, at about 70%: as suggested by Figure 6, the relatively weak H-bonds in this model between the carboxyl of ibuprofen and silanols are easily overcome by vdW interactions between the wall and the rest of the molecule.

The role of dispersion in stabilizing the drug-silica interaction has been confirmed also by simulating a modified S2 structure (not shown here), in which ibuprofen is still H-bonded to the surface but the rest of the molecule points toward the center of the pore. This model is 41 kJ·mol^{-1} less stable than the S2 structure reported in Figure 5. This is an interesting result, since in literature such a "dispersion-free" configuration is usually assumed as the correct geometry of interaction.[16]

In all cases, however, the inclusion of dispersive forces for structures previously optimized with pure B3LYP deeply reshapes the adsorption geometries. The apolar part of ibuprofen moves closer to the wall, as the electronic repulsion is surmounted by vdW attraction. An example of this behavior is reported in Figure 8, where the B3LYP optimized geometry for model S4 is superimposed to the B3LYP-D* structure.

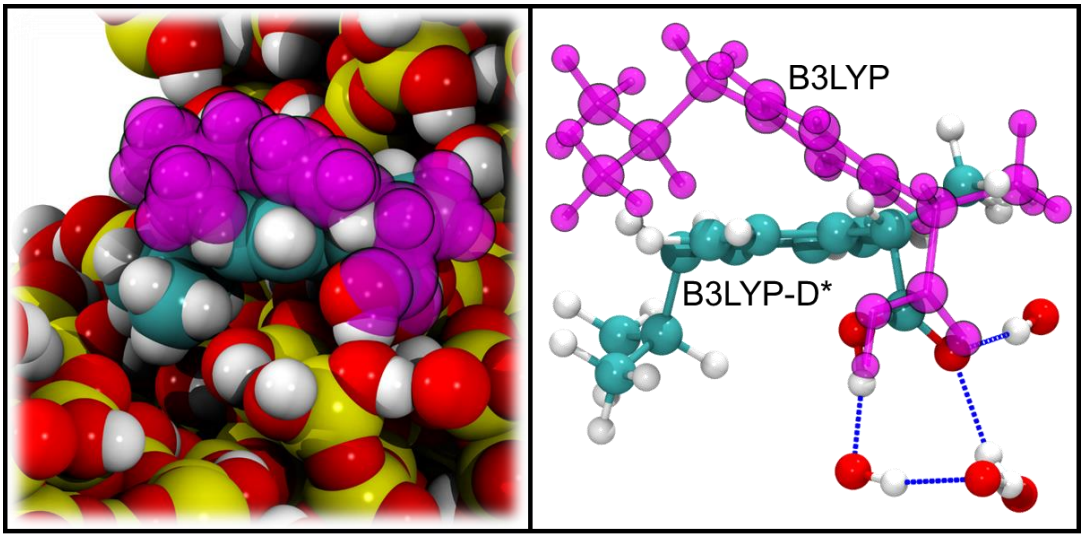

Figure 8. Geometrical effect of dispersion. Space filled (left) and local ball-and-stick (right) structures of ibuprofen adsorption on face S4: B3LYP-D* geometries with superimposed B3LYP structure (magenta).

In a previous work,[20] we have found that for adsorption on a dehydroxylated silica surface, dispersive interactions and H-bonds actively compete, with the former even dominating over the latter. This causes an elongation of the intermolecular H-bond distances to maximize the dispersion interaction of the most hydrophobic part of the drug. The comparison of H-bond lengths between B3LYP and B3LYP-D* models, as reported in Figure 6, does indeed confirm this behavior also for adsorption in MCM-41, despite the model being highly hydroxylated. Length increments are present in all structures except S6. In the S3 case, all H-bonds are longer for B3LYP-D* than for B3LYP. For S5, the effect of dispersion is to bring the ibuprofen C=O group to interact with a different silanol with respect to the B3LYP geometry. These results confirm the competition between the two driving forces of the adsorption. The fact that dispersion here seems prevailing also for a highly hydrophilic silica sample is probably due to the morphology of the material. In Ref.[20] ibuprofen was interacting with a silica surface

model, while here the drug is adsorbed on pore walls, that have a significant curvature and with a much larger amount of silica "mass" per ibuprofen molecule.

Lateral interactions among replicas of the same ibuprofen molecule along the pore axis are in all cases very low (on average, 0.6 and -1.3 $kJ \cdot mol^{-1}$ for B3LYP and B3LYP-D*, respectively).

3.4.2 High Loading

The average interaction energies per ibuprofen molecule computed for the High Loading structure are -39.9 $kJ \cdot mol^{-1}$ for B3LYP and -105.6 $kJ \cdot mol^{-1}$ for B3LYP-D*, with a dispersion contribution of 62.2%. These interaction energies are very close to the average of the energies computed for the Single Loading cases, albeit a bit smaller, probably due to a limited destabilization of the optimal adsorption geometries. Dispersion contribution is somewhat larger (62.2% *vs.* 60.6%), due to the new possible lateral interactions inside the pore.

3.4.3 Thermodynamics

Table 1 reports also the standard enthalpy and free energy of adsorption (ΔH^D and ΔG^D) computed including dispersion. Due to the selected approach (described in the Computational Details), these values are to be taken as estimates and the interpretation reported here is only qualitative.

The computed enthalpy values are slightly smaller than the electronic interaction energies and the order of stability is retained, as expected. Considering ΔG^D values, our calculations predict in all cases a spontaneous adsorption of ibuprofen on the MCM-41 silica walls ($\Delta G^D < 0$). Note that if dispersion had not been considered, all the ΔG^D would have been positive, since the computed $T\Delta S$ (-65.7 $kJ \cdot mol^{-1}$) is larger than all B3LYP ΔE^Ds. The latter consideration demonstrates once more that pure Density

Functional Theory calculations are not suitable to correctly describe such a system where London forces do prevail.

3.5 IR and NMR spectra

For the B3LYP-D* optimized structures of Figure 5 and 7, we have computed experimental observables to be compared with data in literature.

Specifically, the most throughout experimental characterization of ibuprofen confined in MCM-41 is found in Azais *et al.*,[11] where infra-red (FTIR) and magic angle spinning (MAS) ^{1}H, ^{13}C, and ^{29}Si solid-state NMR spectroscopies were used. From their data, authors suggested that, at ambient temperature, ibuprofen is not in a solid state (crystalline or amorphous) and is extremely mobile inside the MCM-41 pores. They also have explained an observed fast drug release from this material in a simulated intestinal or gastric fluid by proposing a weak interaction between ibuprofen and the silica surface.

By our side, as a first step, we have performed a vibrational analysis on both the Single Loading and High Loading structures. As stated in Computational Details, this analysis has been focused solely on the carboxylic functionality of ibuprofen. This choice was justified by the fact that experimentally only the O-H and C=O stretching modes are considered, as other modes are barely affected by the interaction. Figure 9 reports the simulated and experimental[11] IR spectra of ibuprofen both in its racemic crystalline form[53] and encapsulated in the MCM-41 material. Only the region corresponding to the C=O stretching mode is shown. For the simulation, only the High Loading model is included. Experimental spectra are referred to two MCM-41 samples with different pore diameter and no correlation is reported with this geometrical parameter. From Figure 9, right, it can be noticed that drug incorporation has two

effects: a) a bathochromic shift of 12 cm^{-1} with respect to the ibuprofen racemic crystal value and b) a marked broadening of the IR band. The same shift has been recently observed also for ibuprofen interacting with Aerosil® R 816 fumed silica.[54] Another very recent work[16] on ibuprofen confined in MCM-41 has found a bathochromic shift of 8 cm^{-1}, again with a broadening of the signal.

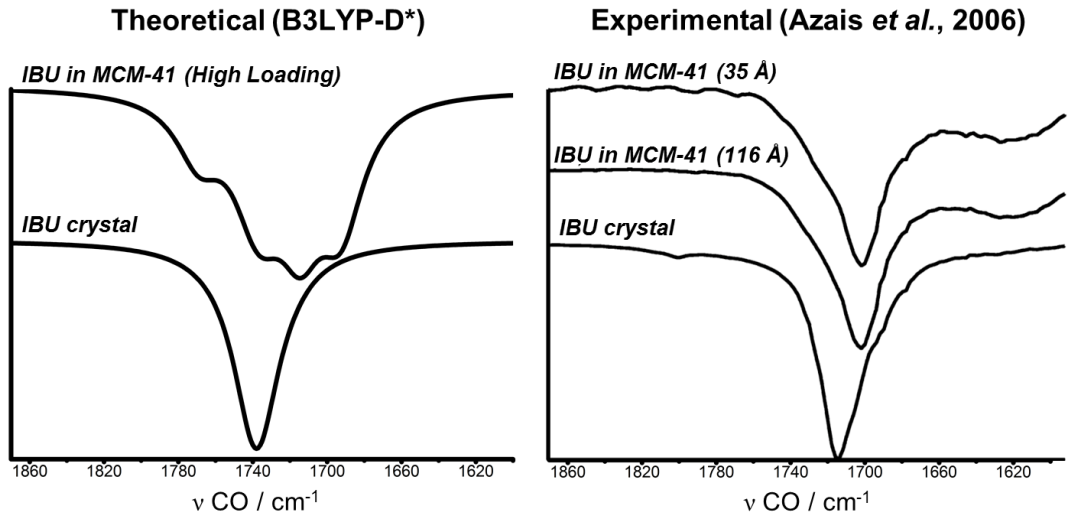

Figure 9. Simulated and experimental infrared spectra of ibuprofen in the C=O stretching mode region. Left: B3LYP-D* simulated spectrum, both for ibuprofen in the High Loading adsorption structure (top) and in the crystal (bottom). Right: experimental spectrum (Adapted with permission from (Azais, T.; Tourne-Peteilh, C.; Aussenac, F.; Baccile, N.; Coelho, C.; Devoisselle, J. M.; Babonneau, F. Solid-state NMR study of ibuprofen confined in MCM-41 material. *Chem. Mater*. **2006**, *18*, 6382-6390). Copyright (2014) American Chemical Society).

Considering our simulations (Figure 9, left), adsorption of ibuprofen inside our MCM-41 model causes a split of the C=O stretching band with respect to the sharp band of the crystal at 1738 cm^{-1}. This splitting covers a broad range of frequencies, each one associated to a different configuration of ibuprofen inside the pore, with the lowest C=O stretching mode at 1692 cm^{-1} and the highest at 1769 cm^{-1}. These results suggest a significant influence of the interaction geometry on the C=O stretching frequency.

Thus, the broadness of the experimental band can be explained with multiple adsorption configurations simultaneously present in the sample, as expected for an amorphous material. Notwithstanding this correlation, most of the computed C=O stretching frequencies (6 out of 7) are equal to or lower than the crystalline case, with an average value of 1723 cm^{-1}. This corresponds to a simulated bathochromic shift of 15 cm^{-1}, remarkably close to the experimental result of 12 cm^{-1} (*vide supra*), especially considering that in our model we are exploring only a limited part of the configurational space. COOH vibrational frequencies for the Single Loading structures (not shown here for brevity) are almost identical to the High Loading case.

Table 2. Assignments of ^{1}H and ^{13}C signals of racemic ibuprofen (CRY), ibuprofen in the High Loading MCM41 model and experimental data of ibuprofen in MCM41 reported by Azais *et al.*[11] Atom numbering from Figure 4.

ATOM	CRY	HL	EXP	ATOM	CRY	HL	EXP
C1	139	140	141				
C2	130	126	130	**H2**	6.9	7.1	6.9
C3	124	123	128	**H3**	7.6	7.5	7.0
C4	132	136	138				
C5	129	126	128	**H5**	6.7	7.0	7.0
C6	124	127	130	**H6**	6.8	7.0	6.9
C7	43	46	45	**H7**	1.5	2.1	2.3
C8	29	32	30	**H8**	1.2	1.5	1.7
C9	23	22	22	**H9**	0.4	0.9	0.7
C10	20	18	22	**H10**	0.2	0.4	0.7
C11	44	47	45	**H11**	1.8	3.6	3.6
C12	13	16	18	**H12**	0.3	1.1	1.3
C13	178	177	180	**H14**	12.5	10.2	13*

*****Extracted from the ^{1}H MAS NMR spectra of ibuprofen/MCM41 recorded at low temperature (183K)

As for NMR calculations, the proton (^{1}H) and carbon (^{13}C) chemical shifts were calculated on the racemic ibuprofen crystal form,[53] on the six Single Loading MCM-41-ibuprofen structures and on the High Loading MCM-41 structure. Figure 10 reports the experimental ^{13}C MAS-NMR spectrum[11] together with the simulated ones for the High Loading case and for the ibuprofen crystal. Figure S2 of Supporting Information includes the ^{13}C simulated spectra also for the 6 Single Loading structures. Table 2 reports the average isotropic chemical shifts of both carbon and proton atoms computed for the racemic ibuprofen crystal form (labeled CRY) and the seven ibuprofen molecules in the HL MCM41 model. All the chemical shifts of protons and carbons for the single loading models are reported in Tables S3 and S4 of the Supporting Information.

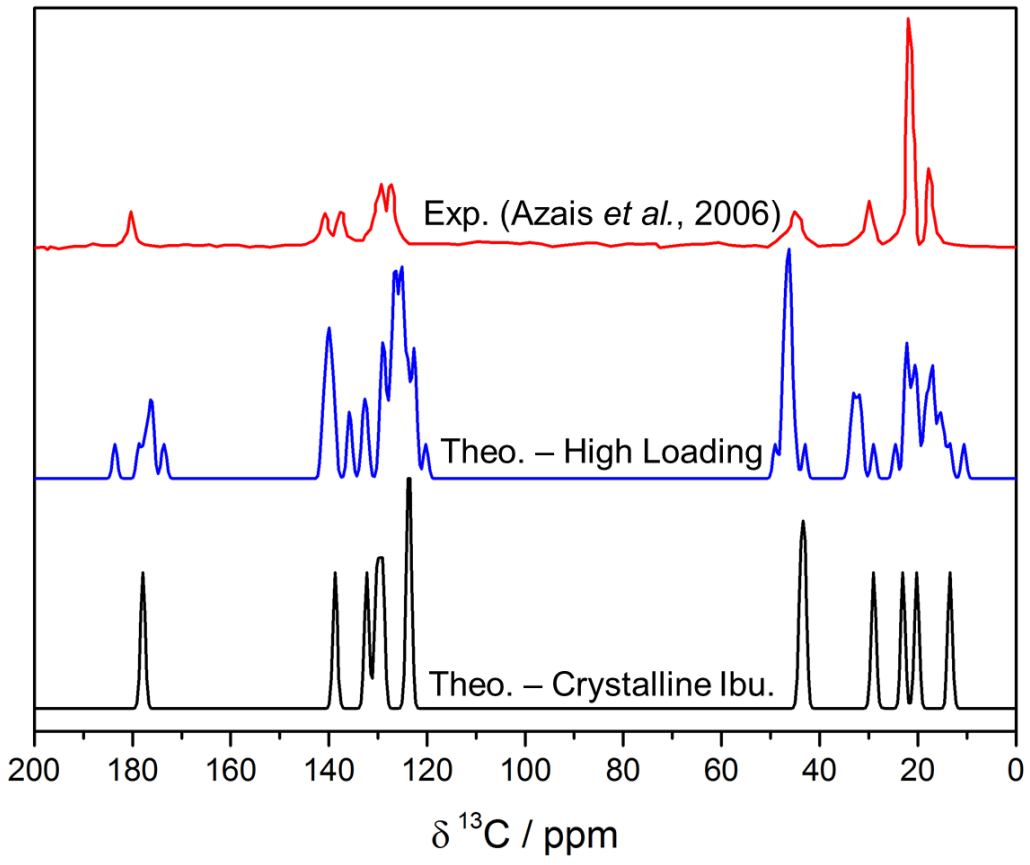

Figure 10. ^{13}C simulated and experimental NMR spectra at the PBE // B3LYP-D* level of theory (see Computational Details). Experimental spectrum (Adapted with

permission from (Azais, T.; Tourne-Peteilh, C.; Aussenac, F.; Baccile, N.; Coelho, C.; Devoisselle, J. M.; Babonneau, F. Solid-state NMR study of ibuprofen confined in MCM-41 material. *Chem. Mater*. **2006**, *18*, 6382-6390). Copyright (2014) American Chemical Society) for ibuprofen encapsulated in MCM-41. Theo. – High Loading refers to the simulated spectrum for ibuprofen in the High Loading case; Theo. – Crystalline Ibu. refers to the simulated spectrum of ibuprofen in its crystalline racemic form.

Both the computed ^{13}C MAS NMR spectra and the assignment reported in Table 2 are in excellent agreement with the experimental counterparts collected by Azais *et al.*[11] Average differences of 2.2 and 0.2 ppm were found on the chemical shifts of carbons and protons, respectively. These results further demonstrate the reliability of our ibuprofen/MCM41 models and the validity of the previously described static calculations.

Considering carbon atoms (Figure 10, S2 and Tables 2 and S3), three distinct families can be identified with respect to the chemical shifts: $\delta < 50$ ppm, corresponding to alkyl carbons; $120 < \delta < 140$ ppm, corresponding to aromatic carbons and δ around 180 ppm, which is the signal of the carboxylic carbon. Passing from the crystal packing to inclusion in MCM-41 causes a notable splitting of all the signals. This suggests that all carbon atoms are perturbed by the interaction and that there is a significant dependence on the geometry of adsorption. Unsurprisingly, the carboxylic carbon is the most perturbed: the unique signal at 177.9 ppm in the crystal is split in 7 different signals in a range of almost 10 ppm when in interaction. However, less expectedly, also the alkyl carbons are greatly perturbed by the interaction and this is due to the strong deformations of the drug apolar portion, described above, that occur to maximize the van der Waals interactions with the pore wall. This signal splitting, in turn, results in a remarkable agreement with the experimental spectrum,[11] also for peak shapes and

intensities. The broadness of the latter has been explained by its authors with a liquid-like nature of ibuprofen in the pores, *i.e.* very high mobility. While this can happen, as also confirmed by more recent experiments by the same group,[14] it is interesting that we were able to partially reproduce the experimental result by just considering 7 different adsorption configurations simulated in a completely static way, *i.e.* without considering any mobility. Nevertheless, it is highly probable that these adsorption structures exhibit a marked mobility at room temperature which, from the present static results, does not seem to have a huge effect on the chemical shifts of the carbon atoms. This topic will be object of a future work.

As regards protons (Tables 2 and S4), while a direct comparison with the experimental spectrum has not been attempted, some clues can still be inferred from the computed chemical shifts. First of all, the proton assignment reported in Table 2 is in perfect agreement with the experimental one. The chemical shifts for the aromatic protons differ, in the various configurations, by less than 1 ppm. The only exception is represented by the signal of the carboxylic proton, which is located at about 10-12 ppm in our models but is not present in the ^{1}H MAS NMR spectra collected at room temperature by Azais *et al.*[11] This discrepancy is explained by the proton exchange involving the proton of the COOH group with that of the silanol groups at the wall pores that occur at ambient temperature and that is not taken into proper account by the static calculations. A deeper investigation of the proton-exchange and of its effects on the ^{1}H chemical shifts should be based on molecular dynamics simulations that intrinsically include thermal effects.[55-57] Indeed, our calculations should be compared with low-temperature ^{1}H MAS NMR experiments which, however, have the drawback of reintroducing the ^{1}H-^{1}H dipolar couplings due to the loss of mobility. By collecting the ^{1}H MAS NMR spectra at 183 K, Azais *et al.*[11] observed the broad ^{1}H signal of the

carboxylic acid group at around 13 ppm which compares fairly well with the 10-12 ppm signals found in the investigated models.

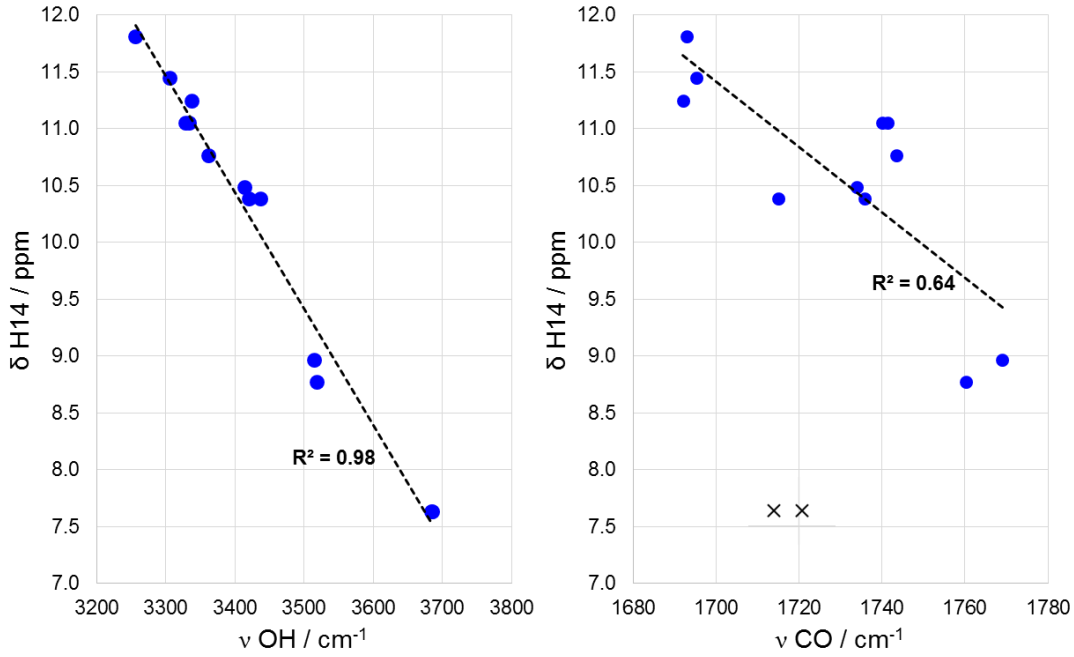

Figure 11. Correlation between the calculated NMR chemical shifts for the carboxylic proton H14 of ibuprofen in the six Single Loading structures (S1-6) and the seven High Loading adsorption positions (HL-1 to 7) and the computed harmonic O-H (Left) and C=O (Right) stretching frequencies. Refer to Table S4 in Supporting Information for the NMR data. Data marked with a cross (X) were not considered in the correlation (see text for more details).

One interesting question is whether a correlation between NMR and IR data exists. On one hand, the chemical shift of the carboxylic proton δ(H14) is a measure of the proton deshielding due to the H-bond donor ability of ibuprofen towards the silica surface. It is therefore not surprising that an almost perfect correlation ($R^2 = 0.98$) exists with the calculated O-H stretching vibrational frequency for all adsorption geometries, both in Single and High Loading (Figure 11, Left). On the other hand, the C=O stretching shift measures the H-bond acceptor ability of the adsorbed ibuprofen. Remarkably enough, a correlation ($R^2 = 0.64$) is also reported between δ(H14) and the

C=O vibrational frequency, as shown in Figure 11 (Right). This suggests that a synergy between H-bond donor/acceptor ability is ubiquitous and robust. Two outliners (marked by an X in figure) have been excluded from this latter correlation. They correspond to structure S5 and its analogue in High Loading (HL5): as stated before, this adsorption geometry is strongly dispersion-driven, with Figure 6 reporting particularly weak H-bonds between this ibuprofen molecule and the surface, with the drug O-H barely interacting with the closest silanol. The fact that for this peculiar structure the aforementioned correlation does not exist is a further hint that the proposed synergy is valid.

4. Conclusions

Providing accurate structures and energy values of drugs interacting with silica can expand our understanding of important processes like drug delivery and degradation of drugs by excipients. To our knowledge, the present paper reports the first all-electron quantum mechanical characterization of a drug confined in a realistic model of mesoporous silica material. This is a topic of great relevance in pharmaceutical research that, however, was missing a detailed insight into the chemistry at its core.

The atomistic details provided by these accurate large-scale simulations allow, for the first time in the literature, to compute the interaction energy of ibuprofen, a key drug in the pharmaceutical field, with MCM-41, a mesoporous silica material which is intensively studied as a drug carrier. Interaction energies are very challenging to be obtained experimentally for this kind of systems (and no such data exist for ibuprofen in mesoporous silica): providing an accurate estimate of their value through quantum mechanical simulation, as we have done here, is of the utmost importance for researchers in the field, interested in tuning these drug delivery systems to maximize

their performance. We also believe that the computed thermodynamics quantities (average adsorption enthalpy and free energy of ΔH = -99 kJ mol^{-1} and ΔG = -33 kJ mol^{-1}, respectively) may be useful to design new functionalized mesoporous silica materials apt to modulate the strength of interaction with ibuprofen and similar drugs. Functionalization of silica based materials is indeed a "hot" topic in the whole bio-inorganic research field.[58]

Our simulations provide a thorough description of the geometrical features of the ibuprofen-MCM-41 interaction, together with a comprehensive analysis of all components of the adsorption energy. We have found that London forces are the driving force of the adsorption, outweighing the local H-bond interactions, in accordance with previous results that were, however, obtained on much smaller and less representative models.[20] The models described here have been validated against experimental observables in literature by comparing both IR and NMR spectra and showing excellent agreement with the experimental counterpart. Our data suggest an alternative explanation to the broadness of the measured specific bands in both NMR and IR spectra, which is based on static disorder of the adsorbed ibuprofen due to slightly different local situation rather than to its dynamic behavior. Our spectroscopic data allowed to suggest a synergy between the H-bond donor/acceptor ability of the adsorbed ibuprofen by showing a correlation between the C=O frequency shift and the δ(H) chemical shift of the acidic proton of the COOH functionality.

Two main limits are affecting these models: the static nature of the simulations and the absence of water. As regards the first problem, *ab initio* Molecular Dynamics (AIMD) on systems of this scale and complexity is computationally very demanding. However, thanks to the improvements in High Performance Computing, these calculations are becoming more and more feasible. We are planning to study the role of

water on the fate of adsorbed ibuprofen, a point relevant to fine tune the pharmacokinetics performance of the system. While AIMD for a full solvated system is still unattainable due to the very long scale time evolution needed to sample the free energy surface, with the present technology some of us have already reported interesting insights on the matter, by focusing on a model of system microsolvation, in which a much reduced number of water molecules competes with ibuprofen for silica surface functionalities.[59]

Acknowledgments

The vast majority of the calculations have been carried out thanks to the PRACE (PaRtnership for Advanced Computing in Europe) project pra50810 "Mesoporous silica for drug delivery: a quantum mechanical simulation" (20 million CPU hours on SuperMUC, LRZ, Munich, Germany). Models have been visualized and manipulated by MOLDRAW[60] and VMD.[61] Progetti di Ricerca di Ateneo-Compagnia di San Paolo-2011-Linea 1A, progetto OR-TO11RRT5 is acknowledged for funding. CRYSTAL developers are acknowledged for providing up to date development versions of the code and fruitful advice. B. Onida (Dipartimento Scienza Applicata e Tecnologia, Politecnico di Torino) is acknowledged for fruitful discussion on the literature experimental data.

References

1. Brash, J. L.; Horbett, T. A. *Proteins at Interfaces: Physicochemical and Biochemical Studies*. ACS Symposium series, 343 ed.; American Chemical Society: Washington, DC, 1987; p. 706.

2. Horbett, T. A.; Brash, J. L. *Proteins at Interfaces II: Fundamentals and Applications*. ACS Symposium Series ed.; American Chemical Society: Washington, DC, 1995; p. 561.

3. Kresge, C. T.; Leonowicz, M. E.; Roth, W. J.; Vartuli, J. C.; Beck, J. S. Ordered mesoporous molecular sieves synthesizad by a liquid-crystal template mechanism. *Nature* **1992,** *359*, 710-712.

4. Corma, A. From microporous to mesoporous molecular sieve materials and their use in catalysis. *Chem. Rev.* **1997,** *97*, 2373-2419.

5. Rimola, A.; Costa, D.; Sodupe, M.; Lambert, J.-F.; Ugliengo, P. Silica Surface Features and Their Role in the Adsorption of Biomolecules: Computational Modeling and Experiments. *Chem. Rev.* **2013,** *113*, 4216-4313.

6. Vallet-Regi, M.; Ramila, A.; del Real, R. P.; Perez-Pariente, J. A new property of MCM-41: Drug delivery system. *Chem. Mater.* **2001,** *13* 308-311.

7. Manzano, M.; Colilla, M.; Vallet-Regì, M. Drug delivery from ordered mesoporous matrices. *Expert Opin. Drug Deliv.* **2009,** *6*, 1383-1400.

8. Wang, S. Ordered mesoporous materials for drug delivery. *Microp. Mesop. Mater.* **2009,** *117* 1-9.

9. Mortera, R.; Fiorilli, S.; Garrone, E.; Verne, E.; Onida, B. Pores occlusion in MCM-41 spheres immersed in SBF and the effect on ibuprofen delivery kinetics: A quantitative model. *Chem. Eng. J.* **2010,** *156*, 184-192.

10. Adams, S. S. The propionic acids: a personal perspective. *J. Clin. Pharmacol.* **1992,** *32*, 317-323.

11. Azais, T.; Tourne-Peteilh, C.; Aussenac, F.; Baccile, N.; Coelho, C.; Devoisselle, J. M.; Babonneau, F. Solid-state NMR study of ibuprofen confined in MCM-41 material. *Chem. Mater.* **2006,** *18*, 6382-6390.

12. Babonneau, F.; Yeung, L.; Steunou, N.; Gervais, C.; Ramila, A.; Vallet-Regì, M. Solid state NMR characterization of encapsulated molecules in mesoporous silica. *J. Sol-Gel Sci. Technol.* **2004,** *31,* 219-223.

13. Bras, A. R.; Merino, E. G.; Neves, P. D.; Fonseca, I. M.; Dionisio, M.; Schonhals, A.; Correia, N. T. Amorphous Ibuprofen Confined in Nanostructured Silica Materials: A Dynamical Approach. *J. Phys. Chem. C* **2011,** *115*, 4616-4623.

14. Guenneau, F.; Panesar, K.; Nossov, A.; Springuel-Huet, M.-A.; Azais, T.; Babonneau, F.; Tourne-Peteilh, C.; Devoisselle, J.-M.; Gedeon, A. Probing the mobility of ibuprofen confined in MCM-41 materials using MAS-PFG NMR and hyperpolarised-129Xe NMR spectroscopy. *Phys. Chem. Chem. Phys.* **2013,** *15*, 18805-18808.

15. Brás, A. R.; Noronha, J. P.; Antunes, A. M. M.; Cardoso, M. M.; Schönhals, A.; Affouard, F.; Dionísio, M.; Correia, N. T. Molecular Motions in Amorphous Ibuprofen As Studied by Broadband Dielectric Spectroscopy. *J. Phys. Chem. B* **2008,** *112*, 11087-11099.

16. Brás, A. R.; Fonseca, I. M.; Dionísio, M.; Schönhals, A.; Affouard, F.; Correia, N. T. Influence of Nanoscale Confinement on the Molecular Mobility of Ibuprofen. *J. Phys. Chem. C* **2014,** *118*, 13857–13868.

17. Ugliengo, P.; Sodupe, M.; Musso, F.; Bush, I. J.; Orlando, R.; Dovesi, R. Realistic models of hydroxylated amorphous silica surfaces and MCM-41 mesoporous material simulated by large-scale periodic B3LYP calculations. *Adv. Mater.* **2008,** *20*, 4579–4583.

18. Coasne, B.; Ugliengo, P. Atomistic Model of Micelle-Templated Mesoporous Silicas: Structural, Morphological, and Adsorption Properties. *Langmuir* **2012,** *28*, 11131-11141.

19. Pedone, A.; Bloino, J.; Barone, V. Role of Host–Guest Interactions in Tuning the Optical Properties of Coumarin Derivatives Incorporated in MCM-41: A TD-DFT Investigation. *J. Phys. Chem. C* **2012,** *116*, 17807-17818.

20. Delle Piane, M.; Corno, M.; Ugliengo, P. Does Dispersion Dominate over H-bonds in Drug-Surface Interactions? The Case of Silica-Based Materials as Excipients and Drug-Delivery Agents. *J. Chem. Theory Comput.* **2013,** *9*, 2404-2415.

21. Grimme, S. Semiempirical GGA-type density functional constructed with a long-range dispersion correction. *J. Comput. Chem.* **2006,** *27*, 1787-1799.

22. Dovesi, R.; Orlando, R.; Erba, A.; Zicovich-Wilson, C. M.; Civalleri, B.; Casassa, S.; Maschio, L.; Ferrabone, M.; De La Pierre, M.; D'Arco, P.; et al. CRYSTAL14: A program for the ab initio investigation of crystalline solids. *Int. J. Quantum Chem.* **2014**, DOI: 10.1002/qua.24658.

23. Bush, I. J.; Tomic, S.; Searle, B. G.; Mallia, G.; Bailey, C. L.; Montanari, B.; Bernasconi, L.; Carr, J. M.; Harrison, N. M. Parallel Implementation of the ab initio CRYSTAL Program: Electronic Structure Calculations for Periodic Systems. *Proc. R. Soc. A-Math. Phys. Eng. Sci.* **2011,** *467*, 2112-2126.

24. Orlando, R.; Delle Piane, M.; Bush, I. J.; Ugliengo, P.; Ferrabone, M.; Dovesi, R. A new massively parallel version of CRYSTAL for large systems on high performance computing architectures. *J. Comput. Chem.* **2012,** *33*, 2276-2284.

25. Lee, C.; Yang, W.; Parr, R. G. Development of the Colle-Salvetti correlation-energy formula into a functional of the electron density. *Phys. Rev. B* **1988,** *37*, 785-789.

26. Becke, A. D. Density-functional thermochemistry. III. The role of exact exchange. *J. Chem. Phys.* **1993,** *98*, 5648-5652.

27. Prencipe, M.; Pascale, F.; Zicovich-Wilson, C. M.; Saunders, V. R.; Orlando, R.; Dovesi, R. The Vibrational Spectra of Calcite ($CaCO_3$): an ab inito Quantum-Mechanical Calculation. *Phys. Chem. Miner.* **2004,** *31*, 559-564.

28. Dovesi, R.; Saunders, V. R.; Roetti, C.; Orlando, R.; Zicovich-Wilson, C. M.; Pascale, F.; Civalleri, B.; Doll, K.; Harrison, N. M.; Bush, I. J.; et al. *CRYSTAL14, User's Manual*. Università di Torino: Torino, Italy, 2014.

29. Monkhorst, H. J.; Pack, J. D. Special Points for Brillouin-Zone Integration. *Phys. Rev. B.* **1976,** *8*, 5188-5192.

30. Nada, R.; Nicholas, J. B.; McCarthy, M. I.; Hess, A. C. Basis Sets for ab initio Periodic Hartree-Fock Studies of Zeolite/Adsorbate Interactions: He, Ne, and Ar in Silica Sodalite. *Int. J. Quantum Chem.* **1996,** *60*, 809-820.

31. Schäfer, A.; Horn, H.; Ahlrichs, R. Fully Optimized Contracted Gaussian Basis Sets for Atoms: Li to Kr. *J. Chem. Phys.* **1992,** *97*, 2571.

32. Broyden, C. G. The Convergence of a Class of Double-rank Minimization Algorithms 1. General Considerations. *IMA J. Appl. Math.* **1970,** *6*, 76-90.

33. Fletcher, R. A new approach to variable metric algorithms. *Comput. J.* **1970,** *13*, 317-322.

34. Shanno, D. F.; Kettler, P. C. Optimal Conditioning of Quasi-Newton Methods. *Math. Comput.* **1970,** *24*, 657-664.

35. Dall'Olio, S.; Dovesi, R.; Resta, R. Spontaneous polarization as a Berry phase of the Hartree-Fock wave function: the case of KNbO3. *Phys. Rev. B* **1997,** *56*, 10105-10114.

36. Yates, J. R.; Pickard, C. J.; Mauri, F. Calculation of NMR chemical shifts for extended systems using ultrasoft pseudopotentials. *Phys. Rev. B* **2007,** *76*, 024401.

37. Pickard, C. J.; Mauri, F. All-electron magnetic response with pseudopotentials: NMR chemical shifts. *Phys. Rev. B* **2001,** *63*, 245101.

38. Giannozzi, P.; Baroni, S.; Bonini, N.; Calandra, M.; Car, R.; Cavazzoni, C.; Ceresoli, D.; Chiarotti, G. L.; Cococcioni, M.; Dabo, I.; et al. QUANTUM ESPRESSO: a modular and open-source software project for quantum simulations of materials. *J. Phys.-Condes. Matter* **2009,** *21*, 395502.

39. Perdew, J. P.; Burke, K.; Enzerhof, M. Generalized gradient approximation for the exchange-correlation hole of a many-electron system. *Phys. Rev. Lett.* **1996,** *77*, 16533-16539

40. Vanderbilt, D. Soft self-consistent pseudopotentials in a generalized eigenvalue formalism. *Phys. Rev. B* **1990,** *41*, 7892-7895.

41. Rappe, A. M.; Rabe, K. M.; Kaxiras, E.; Joannopoulos, J. D. Optimized pseudopotentials. *Phys. Rev. B* **1990,** *41*, 1227-1230.

42. Presti, D.; Pedone, A.; Menziani, M. C. Unravelling the polymorphism of [(p-cymene)Ru(kN-INA)Cl2] through dispersion-corrected DFT and NMR GIPAW calculations. *Submitted to Inorg. Chem.*

43. Pedone, A.; Charpentier, T.; Menziani, M. C. Multinuclear NMR of CaSiO3 glass: simulation from first-principles. *Phys. Chem. Chem. Phys.* **2010,** *12*, 6054-6066.

44. Civalleri, B.; Zicovich-Wilson, C. M.; Valenzano, L.; Ugliengo, P. B3LYP augmented with an empirical dispersion term (B3LYP-D*) as applied to molecular crystals. *Cryst. Eng. Comm.* **2008,** *10*, 405-410.

45. Zhuravlev, L. T. Concentration of Hydroxyl-groups on the Surface of Amorphous Silica. *Langmuir* **1987,** *3*, 316-318.

46. Van Thiel, M.; Becker, E. D.; Pimentel, G. C. Infrared Studies of Hydrogen Bonding of Methanol by the Matrix Isolation Technique. *J. Chem. Phys.* **1957,** *27*, 95-99.

47. Tosoni, S.; Civalleri, B.; Pascale, F.; Ugliengo, P. Hydroxylated crystalline edingtonite silica faces as models for the amorphous silica surface. *J. Phys.: Conf. Ser.* **2008,** *117*, 012026.

48. Brunel, D.; Cauvel, A.; Di Renzo, F.; Fajula, F.; Fubini, B.; Onida, B.; Garrone, E. Preferential grafting of alkoxysilane coupling agents on the hydrophobic portion of the surface of micelle-templated silica. *New J. Chem.* **2000,** *24*, 807-813.

49. Beetge, E.; du Plessis, J.; Müller, D. G.; Goosen, C.; van Rensburg, F. J. The influence of the physicochemical characteristics and pharmacokinetic properties of selected NSAID's on their transdermal absorption. *Int. J. Pharm.* **2000,** *193*, 261-264.

50. Avdeef, A.; Box, K. J.; Comer, J. E. A.; Gilges, M.; Hadley, M.; Hibbert, C.; Patterson, W.; Tam, K. Y. PH-metric logP 11. pKa determination of water-insoluble drugs in organic solvent–water mixtures. *J. Pharm. Biomed. Anal.* **1999,** *20*, 631-641.

51. Mellaerts, R.; Jammaer, J. A. G.; Van Speybroeck, M.; Chen, H.; Humbeeck, J. V.; Augustijns, P.; Van den Mooter, G.; Martens, J. A. Physical State of Poorly Water Soluble Therapeutic Molecules Loaded into SBA-15 Ordered Mesoporous Silica Carriers: A Case Study with Itraconazole and Ibuprofen. *Langmuir* **2008,** *24*, 8651-8659.

52. Vener, M. V.; Egorova, A. N.; Churakov, A. V.; Tsirelson, V. G. Intermolecular hydrogen bond energies in crystals evaluated using electron density properties: DFT computations with periodic boundary conditions. *J. Comput. Chem.* **2012,** *33*, 2303-2309.

53. Shankland, N.; Wilson, C. C.; Florence, A. J.; Cox, P. J. Refinement of Ibuprofen at 100K by Single-Crystal Pulsed Neutron Diffraction. *Acta Cryst.* **1997,** *53*, 951-954.

54. Kołodziejek, J.; Główka, E.; Hyla, K.; Voelkel, A.; Lulek, J.; Milczewska, K. Relationship between surface properties determined by inverse gas chromatography and ibuprofen release from hybrid materials based on fumed silica. *Int. J. Pharm.* **2013,** *441*, 441-448.

55. Gortari, I. D.; Portella, G.; Salvatella, X.; Bajaj, V. S.; van der Wel, P. C. A.; Yates, J. R.; Segall, M. D.; Pickard, C. J.; Payne, M. C.; Vendruscolo, M. Time Averaging of NMR Chemical Shifts in the MLF Peptide in the Solid State. *J. Am. Chem. Soc.* **2010,** *132*, 5993-6000.

56. Dumez, J.-N.; Pickard, C. J. Calculation of NMR chemical shifts in organic solids: Accounting for motional effects. *J. Chem. Phys.* **2009,** *130*, 104701.

57. Barone, V.; Cimino, P.; Pedone, A. An integrated computational protocol for the accurate prediction of EPR and PNMR parameters of aminoxyl radicals in solution. *Magn. Reson. Chem.* **2010,** *48*, S11-S22.

58. Hoffmann, F.; Cornelius, M.; Morell, J.; Fröba, M. Silica-based mesoporous organic-inorganic hybrid materials. *Angew. Chem. Int. Ed.* **2006,** *45*, 3216-3251.

59. Delle Piane, M.; Vaccari, S.; Corno, M.; Ugliengo, P. Silica-Based Materials as Drug Adsorbents: First Principle Investigation on the Role of Water Microsolvation on Ibuprofen Adsorption. *J. Phys. Chem. A* **2014**, DOI: 10.1021/jp411173k.

60. Ugliengo, P.; Viterbo, D.; Chiari, G. MOLDRAW: Molecular Graphics on a Personal Computer. *Z. Kristall.* **1993,** *208*, 383-383.

61. Humphrey, W.; Dalke, A.; Schulten, K. VMD: Visual Molecular Dynamics. *J. Mol. Graph.* **1996,** *14*, 33-38.